Наведено методику CAD/CAE/CAM наскрізного проектування робочого колеса семиступінчастого заглибного насосу марки «ODDESSEzentralasien» – UPP 13-7/6, що застосовується для перекачування сірчаної кислоти в гідрометалургії.

Дослідження проводилися з метою підвищення ККД насоса, що випускається на заводі ТОВ «KARLSKRONA LC AB» (Казахстан). Проведено комп'ютерні розрахунки відцентрового колеса з 8 і 9 лопатками на міцність в CAE системі вищого рівня NASTRAN. Визначено вплив кількості лопаток відцентрового колеса на рівень напружень, що виникають в перетинах лопаток покривного і основного дисків відцентрового колеса. Максимальне напруження в перетинах колеса з 8 лопатями досягло рівня 319 МПа і для колеса з 9 лопатями 199 МПа. Було розглянуто вплив числа лопаток на динамічні характеристики роторного валу. Для цього були змодельовані розрахункові механічні та комп'ютерні схеми динамічного розрахунку для визначення амплітудно-частотних характеристик роторного валу. Амплітуди гармонік на частотах, викликаних пульсацією рідини на лопатковій частоті 400 Гц і 450 Гц, досягли значення $1 \cdot 10^{-4}$ м і $8 \cdot 10^{-4}$ м відповідно. На основі результатів комп'ютерного моделювання статичних і динамічних задач була розроблена модель робочого колеса відцентрового багатоступінчастого насоса з раціональним числом 8 лопатей подвійної кривизни. Вибір кількості лопатей задовольняє критерію міцності колеса, так і критерію динамічності системи вал-колесо.

Для виробництва прототипу колеса був проведений аналіз параметрів технологічного процесу 3D друку по шорсткості поверхні готових виробів. На основі аналізу була вибрана технологія стереолітографії і проведено друкування відцентрових коліс для проведення подальших стендових гідродинамічних випробувань в умовах заводу. Наведені дослідження на основі комп'ютерного моделювання CAD/CAE/CAM дозволяють скоротити часові і матеріальні витрати на розробку геометрії колеса раціональної форми, що задовольняє критерію як міцності самого колеса, так і критерію віброактивності роторного валу

Ключові слова: заглибний насос, відцентрове колесо, системи автоматизованого проектування, амплітудно-частотний відгук

UDC 621.65
DOI: 10.15587/1729-4061.2020.200998

DETERMINATION OF THE RATIONAL NUMBER OF BLADES OF THE CENTRIFUGAL WHEEL OF A SUBMERSIBLE PUMP

M. Isametova
PhD, Associate Professor*
E-mail: isametova69@mail.ru
D. Karaivanov
Doctor of Technical Sciences, Associate Professor
Department of Applied Mechanics
University of Chemical Technology and Metallurgy
St. Kliment Ohridski blvd., 8, Sofia, Bulgaria, 1756
E-mail: dipekabg@yahoo.com
R. Nussipali
Doctoral Student*
E-mail: rollan_n@mail.ru
*Department of Industrial Engineering
Satbayev University
Satpaev str., 22a, Almaty,
Republic of Kazakhstan, 050013

Received date 24.02.2020
Accepted date 15.04.2020
Published date 24.04.2020

1. Introduction

In industrialized countries, centrifugal pumps of various designs are used in many industries; their number and unit capacity are increasing.

The task of designing pumping equipment is complicated by the fact that until now, a sufficiently rigid relationship has not been established between almost all the parameters of the CPs, which are structurally variable, operational (technical), vibrational, technological, etc. One of the important parameters is the number of impeller blades and their optimal choice should be based on hydraulic calculations, for structural reasons, as well as taking into account the strength and dynamic characteristics of the wheel [1, 2].

Determination of the number of blades of the working bodies of the central heating system is based on hydraulic calculations: if the number of blades is small, the blades are overloaded (high flow rates, cavitation, etc.), with a large number of blades, there is a narrowing of the inter-blade channels and an increase in friction. However, hydraulic calculations are not related to the dynamic properties of the rotor, and certainly can not serve as a convincing explanation for the decrease in the strength of the centrifugal wheel and the dynamic properties of the rotor shaft.

To solve this multicriteria problem, it is productive to use the CAD/CAE/CAM method of end-to-end design. Computer simulation of the CAD geometry of the wheel, calculated on the basis of fluid flow hydraulics, allows the strength and dynamic characteristics of centrifugal wheels with a variable number of blades to be determined in the CAE system.

The final in this cycle of design work is the use of CAM systems, that is, the possibility of creating a prototype of the wheel when the image of the product is not completely determined and the use of expensive equipment for manufacturing is extremely expensive. Prototypes of centrifugal wheels allow hydrodynamic tests on stands under production conditions to determine the pressure characteristics of the pump.

The relevance of the work is that the design and improvement of centrifugal pumps is an important production task, the successful solution of which leads to an increase of performance of this equipment.

2. Literature review and problem statement

In [3], the results of research to determine the influence of the number of blades on the flow kinematics in the centrifugal wheel of a single-stage pump are presented. It is shown that wheels with the number of blades 5 and 9 have higher flow friction inside the channels, and the most optimal is a wheel with 7 blades. However, there are still unresolved issues related to the strength of the centrifugal wheel and the increase in its metal content. In [4], the mutual influence of the number of wheel blades 5, 6, 7 and the number of diffuser blades 8, 9, 10 was considered. As a result of research based on numerical modeling, it was found that the case 7+8 has a minimum wheel oscillation, but the influence of pulsation of the forces on the rotor - wheel system was not identified, and this is important, since the dynamic characteristics of the rotor affect both the efficiency value and the strength of the shaft as a whole.

The approach of selecting the wheel by strength parameters was used in [5], but it was based only on variations in the speed of rotation of the rotor shaft, but not on the influence of flow pulsation and the strength of the centrifugal wheel, which depends on the choice of the number of blades.

In [6], studies of failure processes of engineering units of a centrifugal pump are presented. The study is based on the analysis of rotor shaft fatigue using a modified Goodman test. The authors of the paper [7] gave results on the study of the influence of the natural frequencies of vibrations of the centrifugal wheel on the strength of the shaft caused by the difference in the number of wheel blades and the diffuser. The work [8] was devoted to calculating the strength of disks based on the use of a modified method of successive approximations in displaced Chebyshev polynomials. In [9], it was found that the destruction of the impellers of pumping units in the form of cracks and chips in most cases occurs due to fatigue failure of the metal. The dependence of the fatigue life of the impeller made of 25L steel on the influence of the pumped medium was determined.

In all these works, insufficient attention was paid to the study of the influence of the number of blades, both on the strength of the wheel itself and on the dynamic characteristics of the rotor shaft. All this suggests that it is advisable to conduct a study to determine the optimal number of blades that meet the criteria for the strength of the centrifugal wheel and the dynamics of the shaft of a multi-stage pump.

3. The aim and objectives of the study

The purpose of the study is to determine the optimal number of blades of the centrifugal wheel of a submersible centrifugal pump. This will make it possible to design a centrifugal pump with improved performance indicators, such as strength, durability and high efficiency.

To achieve this goal, the following objectives were set:

– create a design mechanical scheme for static and dynamic calculation of the wheel of a seven-stage centrifugal pump;

– perform calculations on the strength and amplitude-frequency response of the rotor-wheel system;

– conduct a comparative analysis of the strength and dynamic characteristics of centrifugal wheels with 8 and 9 blades;

– choose a technology for growing parts in layers and create a prototype of a centrifugal wheel with an optimal number of blades.

4. Research materials and methods

The object of the study is the centrifugal wheel of a vertical submersible seven-stage pump for pumping sulfuric acid into a uranium well.

Input data for pump design:

– Q (feed)=13 meter cubic per hour;

– N (head)=55 meter;

– N (number of revolutions of the electric motor)=2850 rpm;

– i_Q (number of flows)=1;

– i_H (number of stages)=7.

At the CAD stage, an automated module to perform hydrodynamic calculations and profiling the channel of the wheel and the blade was created in the mathematical environment of MATLAB. The algorithm for drawing the profile of the blade includes the determination of its geometry through the Cartesian coordinates, which are specified as a function of the circumference and radius of the wheel, defined in cylindrical coordinates.

$$x_i = r_i \cdot \cos\theta_i;\ y_i = r_i \cdot \sin\theta_i, \tag{1}$$

where x_i, y_i – coordinates of the points belonging to the profile of the blade, r_i – corresponding to the coordinate, θ_i – the angle of coverage corresponding to the coordinate.

This created algorithm allows you to accurately draw the geometry of the designed cylindrical blade in any CAD system. Fig. 1 presents the user interface windows of an automated module.

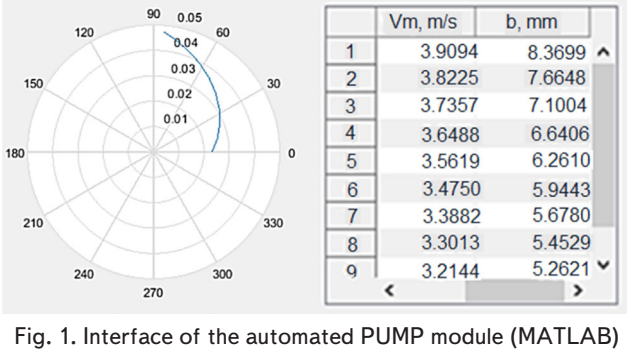

	Vm, m/s	b, mm
1	3.9094	8.3699
2	3.8225	7.6648
3	3.7357	7.1004
4	3.6488	6.6406
5	3.5619	6.2610
6	3.4750	5.9443
7	3.3882	5.6780
8	3.3013	5.4529
9	3.2144	5.2621

Fig. 1. Interface of the automated PUMP module (MATLAB) with calculated data

When designing a centrifugal wheel, the number of blades is determined by the formula

$$z_i = 6.5 \cdot \frac{r_1 + r_2}{r_2 + r_1} \cdot \sin\frac{1}{2}(\beta_1 + \beta_2), \tag{2}$$

where r_1 is the radius of the midpoint of the width of the blade at the inlet, r_2 is the radius of the wheel rotor at the output, β_1, β_2 – input and output angle of the blade

In the analytical calculation z_i=8.5, to create a pump design with increased performance indicators, the question of choosing the number of blades between the number 9 and 8 arises.

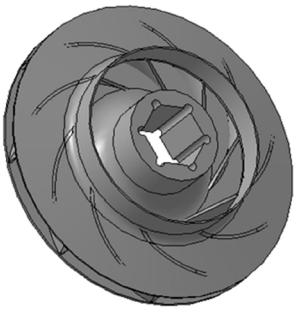

Fig. 2. 3D model of the designed wheel with double curvature blades

Fig. 2 shows the 3D model of the designed wheels with nine blades. The geometry of the impeller with a cylindrical blade has been optimized by creating a double curvature blade. The impeller blade of double curvature allows the stage to work with greater efficiency while maintaining the pressure in comparison with a cylindrical blade, and the larger the feed, the more noticeable it is. The choice of optimal velocity ratios and the optimal appropriate form of the flow part are one of the main ways to significantly improve the performance of a submersible centrifugal pump stage.

5. Creation of a design mechanical scheme for static and dynamic calculation

The task of checking the static strength of the wheels in two versions is to determine the stresses arising under the action of operational loads. Comparison of stresses arising in the sections of the wheel, with allowable stresses allows us to evaluate the performance of the construction. Evaluation of the strength of the wheel can also be done by comparing the working frequency of the rotor with the frequency of rotation at which the damage of the disk or a sharp increase in its size due to the fluidity of the material. The performance of the disk should be estimated by equivalent stresses, the determination of which is possible by the numerical finite element method.

To study the influence of the number of blades on the strength of the wheel and on the dynamics of the rotor, a NASTRAN/PATRAN highest level computer-aided design system was chosen [10, 11].

5. 1. Grid generation

The wheel model was imported from the CAD system, since the wheel was created as an assembly of elements (cover disk, main disk and 9 blades), the "Boolean" operation was used in the PATRAN preprocessor to combine all parts, so such created computer model corresponds to the manufacturing technology of the wheel. The mesh was approximated by eight-node TET structural elements; to generate a detailed mesh the element size was chosen from the condition of the smallest size of the wheel wall thickness of 0.001 m.

The dimension of the problem with such a value of the face of the finite element is 256,000 elements.

Fig. 3 shows the finite element grid of a centrifugal wheel with 9 blades.

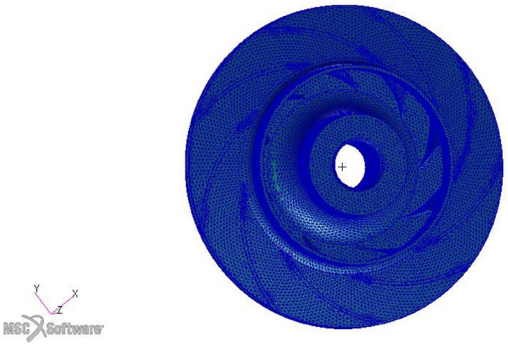

Fig. 3. Finite element wheel model

5. 2. Operating conditions for static analysis

The strength calculation of the impeller of a submersible centrifugal borehole pump includes the calculation of the blades tension from the action of centrifugal forces and the calculation of the disks tension from the action of fluid pressure on the front and rear of the cover and main disks [12, 13].

The calculation of blades tension is in the determination of the stress caused by centrifugal force. For blades that have a constant cross-sectional area, the centrifugal force is found by the formula [14]:

$$F_C = \rho \cdot \omega^2 \cdot F \frac{\left(R^2 - r^2\right)}{2}, \quad (3)$$

where R and r are the outer and inner radius of the blade, respectively, m.

The scheme of application of centripetal forces is shown in Fig. 4.

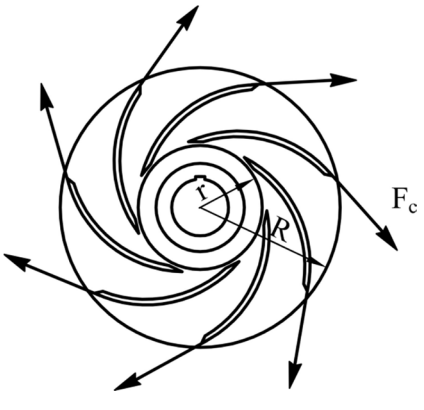

Fig. 4. Computational scheme for the static analysis of the wheel RAS in the plane perpendicular to the axis of rotation

In the process of calculation, the total impact of centrifugal forces arising from the rotation of the wheel and the influence of fluid pressure on the walls of the disks on the impeller was taken into account [15, 16].

When modeling the computational scheme, it must be taken into account that the pressure distribution over the surfaces of the impeller disks is not constant, but depends on the form of fluid movement in the sinuses of the stage. In this case, finding the pressure distribution over the surfaces of the impeller disks is reduced to solving the problem of

the relative liquid rest in a rotating coordinate system. The pressure in the gap between the wheel and the casing (on the front or rear disk) $p(r)$ will be the sum of the pressure at the wheel outlet p_2 and the pressure $p_\omega(r)$, due to the action of centrifugal force on the liquid [17, 18].

For a uniform rotation of the liquid, two mass forces act on its elementary volume: gravity and centrifugal inertia of the liquid.

In a centrifugal pump, the angular velocity of the rotor is so great that gravity can be neglected compared to centrifugal force. Then the differential hydrostatic equation will have the following form

$$dp = \rho\left(\omega_l^2 \cdot x \cdot dx + \omega_l^2 \cdot y \cdot dy\right). \quad (4)$$

From (4) by integration we obtain the law of pressure distribution, which has a parabolic shape

$$p(r) = \frac{\rho \cdot \omega^2}{8} r^2 + C. \quad (5)$$

The integration constant C is defined from the condition that the pressure on the radius r_2 is equal to the pumping pressure p_2, then

$$p(r) = p_2 + \frac{\rho\omega^2}{8}\left(r^2 - r_2^2\right). \quad (6)$$

In formula (6), the first term is the outlet pressure, the second term is the pressure due to the action of centrifugal force on the liquid.

Centrifugal pumps are assembled as multi-stage to increase the pressure. Such a pump is a series of single-stage pumps, the impellers of which are settled on a common shaft and are connected in series (Fig. 5).

From (4) by integration we obtain the law of pressure distribution, which has a parabolic shape.

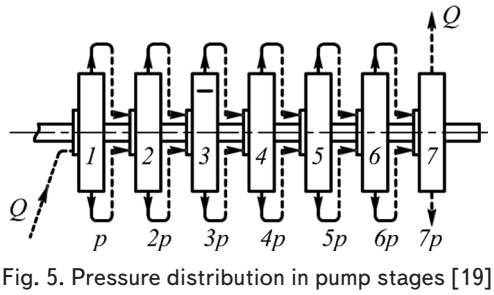

Fig. 5. Pressure distribution in pump stages [19]

In this case, the head created by each wheel is added and the total head of the injector is equal to the sum of the heads of the separate stages. According to the pressure distribution scheme in the pump (Fig. 6), the wheel of the sixth section is the most loaded.

Taking into account the above, to test the influence of the number of blades on the strength of the wheel, the sixth stage of a centrifugal multistage pump was selected. For strength calculation of the wheel of the sixth stage, the design scheme is presented in Fig. 7.

The pressure at the inlet P_5 and at the outlet P_6 was determined by the formula expressing the dependence of pressure on the developed pressure:

$$P_i = \rho \cdot g \cdot H_i, \quad (7)$$

where P_i, H_i are pressure and head of i-th stages, respectively, ρ is the density of the flowing liquid, and g is the acceleration of gravity.

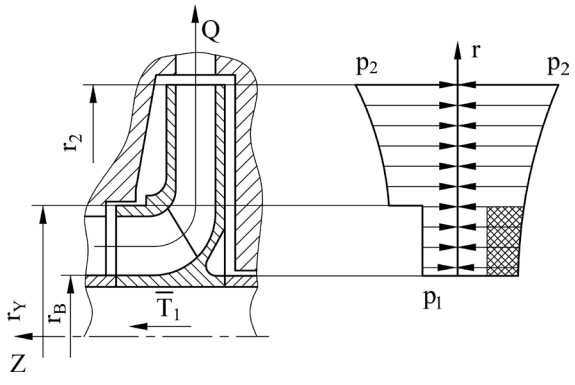

Fig. 6. Pressure distribution on both sides of the wheel (blade pumps)

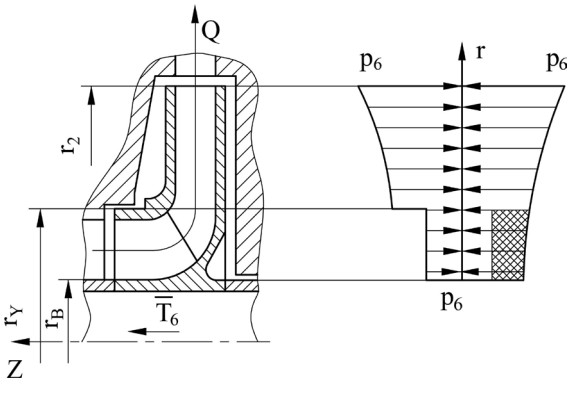

Fig. 7. Loading scheme of the centrifugal wheel of the sixth stage

The input data for the static calculation are listed in Table 1.

Table 1

Input data for the static calculation

No.	Parameter	Value
1	Material	steel
2	Modulus of elasticity E	$2 \cdot 10^{11}$ Pa
3	Poisson's ratio	0.3
4	Support 1	Swivel hinge with rotation about an axis
5	Support 2	Swivel hinge with rotation about an axis
6	P_5 – pressure at the inlet of the wheel	0.4 MPa
7	P_6 – pressure at the outlet of the wheel	0.56 MPa
8	F_c – centrifugal force	24.19 N
9	Calculation Type	Static Solver 120

In the settings of Solver 120, the CASI parameter was selected, which allows calculating large-size tasks from solid elements.

6. Calculations of the amplitude-frequency response of the rotor-wheel system

In order to really simulate the pressure changing over the surface of the wheel disks, we used the Spatial Field application, which describes a data set that changes according to the real set in the Cartesian or cylindrical coordinate system. Considering the main modeling condition that the computer model must be adequate to the wheel's functioning conditions, the second term in analytical formula 3 will be represented through the Spatial Field, which expresses the dependence of the pressure of the centrifugal forces of the liquid on the radius of the wheel.

In order not to violate the symmetry of the location of the support, when creating the boundary conditions for the displacements of the wheel, RBE2 elements were used [20].

To perform the static calculation, the Solver120 solver was chosen, the Cassio solver settings allowed to reduce the calculation time.

6. 1. Operating conditions for dynamic analysis

The CP operation is based on the transfer of mechanical energy of a liquid during the force action of the blades on it. During operation, all the parts of the CP are affected by dynamic influences of a different nature. A change in the mode of operation of the central nervous system is accompanied by a change in load. The determination of dynamic effects is necessary to consider the issues of strength and forced oscillations of the rotor of the CP rotor.

In [21], the influence of radial force on the rotor at the blade frequency was found out

$$f_r = f \cdot z, \tag{8}$$

where f_r is the blade frequency, f is the rotation frequency, z is the number of centrifugal impellers.

The problem of choosing the optimal number of centrifugal impeller blades was solved based on the dynamic characteristics of the rotor, i. e., the amplitude-frequency response of the system to the influence of the hydrodynamic force F_r at a frequency of 400 Hz (8 blades), and a frequency of 450 Hz (9 blades).

The task of determining the AFC of the pump rotor is reduced to calculating the eigenvalues of the frequencies ω_0, the modes of natural vibrations at the corresponding value of the frequency ω_0, and a further study of the resonant states of the rotor of the AFC of the CP is studied in the range of eigenfrequencies of the oscillation of the rotor.

For the given boundary conditions in the FE model, the eigenfrequencies of the rotor were determined using the Lanczos method [22]. The data on the first six modes are shown in Table 2.

Table 2

Data on the first six modes

Rotor Waveform	Results	
	The form	Frequency of free oscillations Hz
1st form	Torsional	200
2nd form	Bending	1,300
3rd form	Bending	1,393
4th form	Torsional	2,089
5th form	Bending	3,455
6th form	Bending	3,460

Forced vibrations of the CP are convenient to be represented graphically in the form of AFC for the identification of which it is necessary to solve the equation

$$[\mathbf{M}]\cdot\{\ddot{q}\}+[\mathbf{B}]\cdot\{\dot{q}\}+[\mathbf{C}]\cdot\{q\}=\{F(t)\}, \tag{9}$$

where [M], [**B**], [**C**] – matrix of masses (inertia), damping and system rigidity; $\{\ddot{q}\}$, $\{\dot{q}\}$, $\{q\}$ – generalized movements of nodes and their derivatives; ($F(t)$} –generalized forces [23].

In matrix form, we represent equation (9) as

$$\begin{bmatrix} [m^{(1)}] & [0] & \dots & [0] \\ [0] & [m^{(2)}] & \dots & [0] \\ \dots & \dots & \dots & \dots \\ [0] & [0] & \dots & [m^{(n)}] \end{bmatrix} \begin{Bmatrix} \{\ddot{q}^{(1)}\} \\ \{\ddot{q}^{(2)}\} \\ \dots \\ \{\ddot{q}^{(n)}\} \end{Bmatrix} + \begin{bmatrix} [b^{(1)}] & [0] & \dots & [0] \\ [0] & [b^{(2)}] & \dots & [0] \\ \dots & \dots & \dots & \dots \\ [0] & [0] & \dots & [b^{(n)}] \end{bmatrix} \begin{Bmatrix} \{\dot{q}^{(1)}\} \\ \{\dot{q}^{(2)}\} \\ \dots \\ \{\dot{q}^{(n)}\} \end{Bmatrix} + \begin{bmatrix} [c^{(1)}] & [0] & \dots & [0] \\ [0] & [c^{(2)}] & \dots & [0] \\ \dots & \dots & \dots & \dots \\ [0] & [0] & \dots & [c^{(n)}] \end{bmatrix} \begin{Bmatrix} \{q^{(1)}\} \\ \{q^{(2)}\} \\ \dots \\ \{q^{(n)}\} \end{Bmatrix} = \begin{Bmatrix} \{F^{(1)}(t)\} \\ \{F^{(2)}(t)\} \\ \dots \\ \{F^{(n)}(t)\} \end{Bmatrix}. \tag{10}$$

For the mathematical model of forced vibrations represented by equation (9), the corresponding computer model will be implemented by entering data, such as the mass of the rotor [**M**] with mounted seven wheels, the structural damping coefficient [**B**], the system rigidity [**C**], which depends on the module the elasticity of the steel 40X (40Cr) material and from the wheel parts cross sections geometry, the component $F(t)$ w ill be described by the amplitude, i. e. the value of the hydrodynamic radial force and the pulsation frequency of this force equal to 400 Hz and 450 Hz for eight and nine centrifugal blades, respectively.

The hydrodynamic radial force acting on the CP rotor is divided into two components: static and dynamic. The static component of the radial force is a force averaged over time. The dynamic component of the radial force is caused by the non-stationary flow in the flowing part of the guide apparatus and causes pulsations of pressure and fluid velocity [24]. The direction and magnitude of the radial force are shown in Fig. 8.

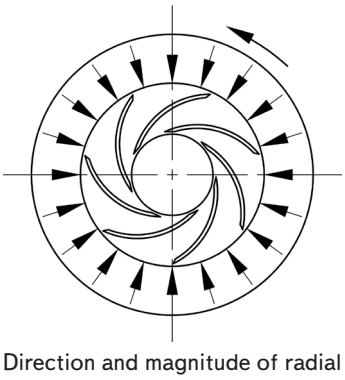

Fig. 8. Direction and magnitude of radial forces

The complex nature of the spatial flow in the flow part of the pump and the viscous properties of the pumped liquid do not allow to determine an accurate analytical dependence of the radial force on the feed. Therefore, analytical dependences of the radial force value on the feed of the CP are obtained on the basis of experimental data and the adopted simplifications. The derivation of the analytical formula of radial force is presented in the paper. For an approximate calculation of the radial force, one uses the following dependence [25]

$$F_r = K_r \cdot p \cdot g \cdot H \cdot D_2 \cdot b_2, \quad (11)$$

where K_r – radial force coefficient, (K_r=0.36); D_2 – outlet wheel diameter, D_2=0.515 meters; b_2 – outlet wheel width, b_2=0.111 meters; p – fluid density, p=1,000 kg per meter cubic; g – gravity acceleration; H – current head, meters.

Input data and boundary conditions for determining the effect of the number of centrifugal impeller blades on the frequency response of the rotor were summarized in Table 3.

Table 3

Input data and boundary conditions for determining the effect of the number of centrifugal impeller blades

No.	Parameter	Value
1	Material	steel
2	Modulus of elasticity E	$2 \cdot 10^{11}$ Pa
3	Poisson's ratio	0.3
4	Steel density	1,500 kg per m^3
5	Support 1	Swivel hinge with rotation about an axis
6	Support 2	Swivel hinge with rotation about an axis
7	F_r – radial hydrodynamic force	105 N
8	F_u – radial force from the wheel disbalance	24.19 N
9	F_a – axial force	1.2 kN
10	Calculation Type	Static Solver 120 DynamicSolver122

Fig. 9 shows a finite element model of the rotor with supports modeled using the RBE2 elements option.

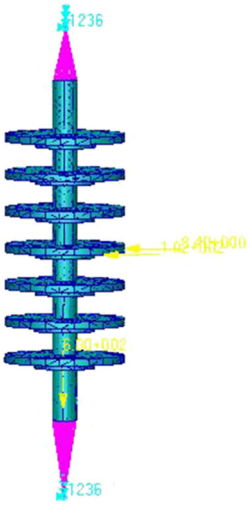

Fig. 9. Finite element model of the rotor

Using the superposition principle, the radial forces acting on each pump stage were modeled as a concentrated force applied at the center of the rotor shaft.

7. Comparative analysis

The task of testing the static strength of the disk is to determine the stresses arising under the action of operational loads. Comparison of them with permissible stresses allows us to evaluate the performance of the construction. In this setting, the task is the content of the verification calculation of the strength of the disk. The calculation results for centrifugal wheels with 8 and 9 blades are not shown in Fig. 10. The maximum stress in a centrifugal wheel with 9 blades is σ_{max}=199 MPa, and the stress level in the wheel with 8 blades reached σ_{max}=319 MPa.

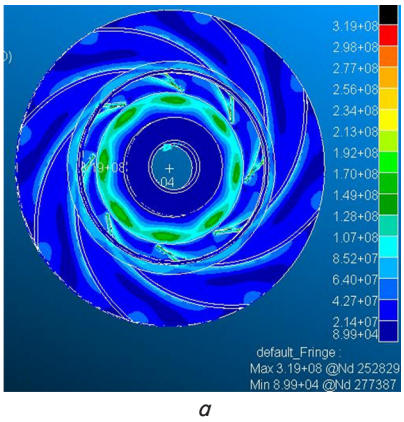

a

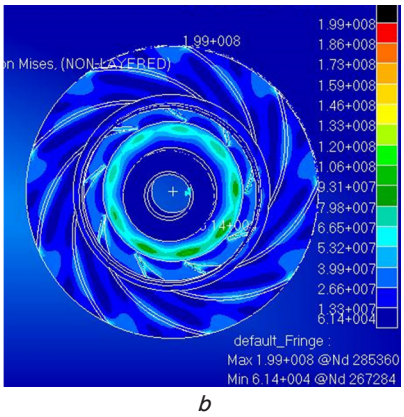

b

Fig. 10. Tension diagrams: *a* – in a wheel with eight blades; *b* – in a wheel with nine blades

In addition, the stress distribution image showed the most dangerous places in the wheel, it is the junction of the blades and disks, which corresponds to the observation given in. Fig. 11 shows the adequacy of the computer model of the physical model of the places of maximum stress concentration.

Since the task of choosing the number of blades is multifactorial, in order to clarify the effect of this parameter on the vibratory activity of the rotor shaft, the results of dynamic calculation on determining the amplitude-frequency characteristics of the rotor were analyzed.

As a result of calculating the static strength of the shaft in the NASTRAN program, equivalent stresses (Fig. 12, *a*) and values of static deflections of the shaft (Fig. 12, *b*) are obtained.

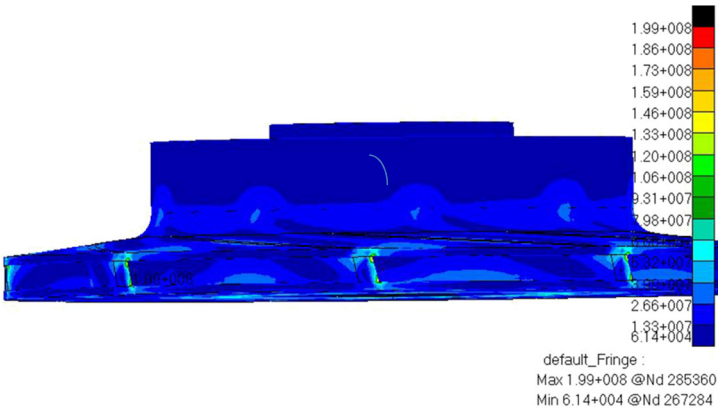

a

b

Fig. 11. Concentrations of tension in the wheel:
a – distribution of maximum stresses in the wheel;
b – breakdown of centrifugal wheels

Analysis of the results showed a sufficient safety factor at maximum feed, according to the diagram σ_{max}=34.6 MPa, δ_{st}=9,2·10^{-5} m the permissible stress for steel [σ_]=450 MPa, the coefficient of safety is 10, 2.

In the frequency range under consideration, one harmonic appears at the lowest frequency equal to 1,330 Hz, and the fifth eigenfrequency appears at a higher frequency of 3,560 Hz, which can be ignored. The value of the oscillation amplitude of the rotor is δ=2·10^{-3} m (Fig. 12, the blue line is for the node in the center of the rotor).

The resonant states of the rotor of the central oscillator frequency response were studied in the eigenfrequency range of the oscillation of the rotor at 4,000 Hz, the influence of the hydrodynamic force F_r at a frequency f_r=450 Hz is shown in Fig. 13, the frequency corresponding to nine blades in a centrifugal wheel.

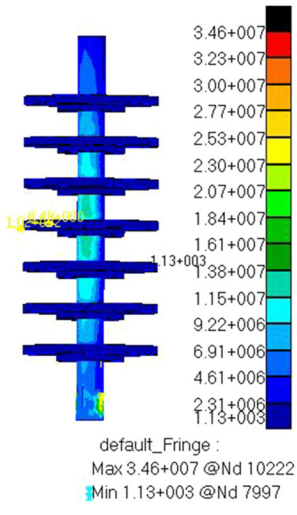

a

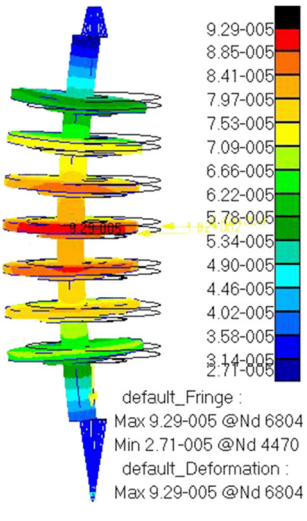

b

Fig. 12. Static strength of the rotor in the maximum feed mode: *a* – equivalent stresses;
b – displacement plot

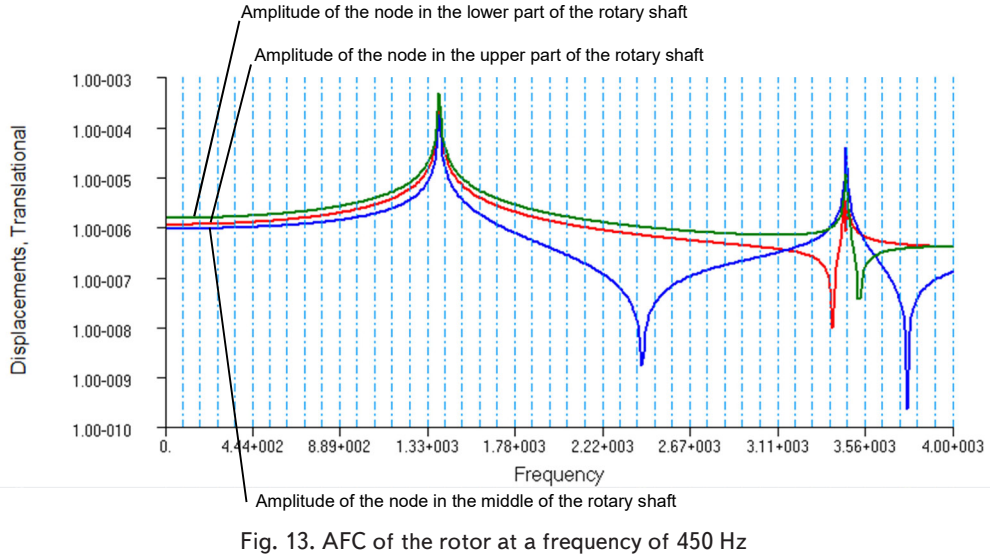

Fig. 13. AFC of the rotor at a frequency of 450 Hz

When the number of blades of a centrifugal wheel is eight, the response of the system to the influence of hydraulic force at a blade frequency of 400 Hz is presented in the AFC diagram in Fig. 14.

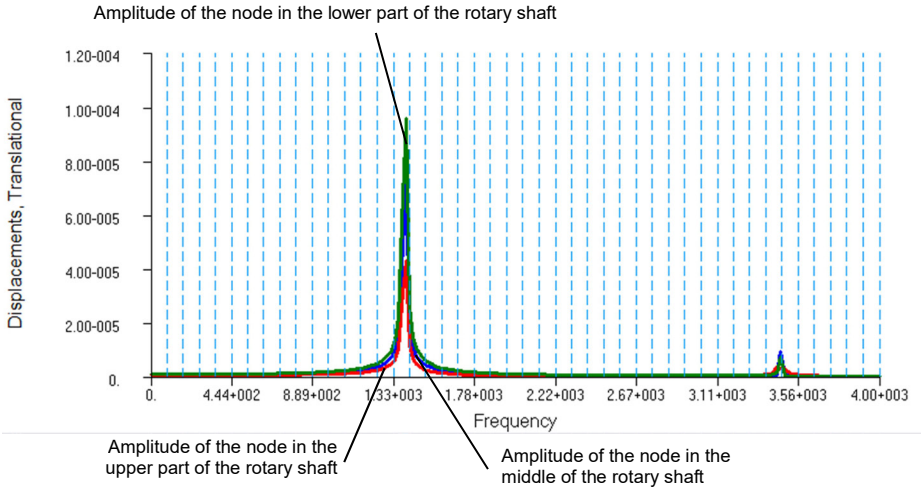

Fig. 14. AFC of the rotor at a frequency of 400 Hz

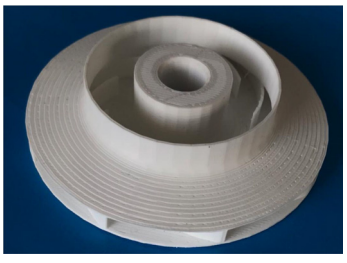

a

b

Fig. 15. Prototypes of the impeller: *a* — prototype printed using FDM technology; *b* — prototype printed using SLA technology

In the diagram above, two harmonics are shown at a frequency of 1,330 and 3,560 Hz, and at the lowest frequency a maximum peak of an amplitude occurs as equal to $\delta=1\cdot10^{-4}$ m.

Analyzing the influence of the number of blades on the stress state of the wheel, safety factors k were found as follows: for nine blades $k=2.19$, for eight blades $k=1.4$, which are identified sufficient for the case.

8. CAM design, prototype centrifugal wheels creation

When creating a prototype of a centrifugal wheel, close to the real model, the primary factor was the selection of 3D printing technology by roughness parameter. When choosing SLA technology that works with liquid photopolymer (stereolithography), the author's data [28], given in Table 3, were taken into account.

In accordance with the manufacturing technology and the requirements applied to the parts of the centrifugal submersible pump stage, an absolute roughness of up to 0.3 mm is permissible for the inner surfaces of the structural elements.

An important parameter that determines the quality of the surface is the quality of the original three-dimensional CAD-model. The virtual model is a 3D surface in the form of a closed grid of triangles. The surface roughness directly depends on the quality of the grid. Thus, when using a low-quality three-dimensional model, macro scale roughness (Fig. 15, *a*), indicated in the simulation data file, can appear when building a physical model and give unreliable results of the quality of the printer or the effectiveness of the selected technology. Fig. 15 shows model prototypes printed using FDM and SLA technologies [29].

The prototypes of centrifugal wheels make it possible to conduct hydrodynamic tests to test the pressure characteristics of the designed wheel, which leads to savings in production costs for the manufacture and equipment, so equipment for the manufacture of a centrifugal wheel costs the company $ 150,000.

9. Discussion of computer analysis results

Based on this analysis, we conclude that a wheel with eight blades, despite a higher rate of stresses, has a sufficient margin of safety, and pulsation of hydrodynamic force in the channels of such a wheel causes a lower amplitude-frequency response, therefore, for the prototype manufacture model with eight blades is chosen.

Analysis of the AFC diagrams of the rotor for the blade frequencies of 400 Hz and 450 Hz allows to choose 8 blade impellers, because the diagram in Fig. 13 has 4 harmonics with the largest amplitude of 810^{-4} m, while the diagram in Fig. 9 indicates the occurrence of two harmonics with a maximum amplitude of 110^{-4} m (Fig. 12, 13), that is, the dynamic forces that occur when the 9-blade wheel causes a large vibration activity of the rotor, which leads to a loss of efficiency and a reduction in the service life of the technological system.

The authors in [26, 27] propose to evaluate the dynamic gain coefficients as indicators of vibration activity of the shaft. Analyzing the frequency spectra of vibration (Fig. 12, 13), we determine the coefficient of dynamic gain at resonance. The coefficient $\eta=\frac{\delta}{\delta_{st}}$ is determined by the ratio of the amplitude of the forced harmonic vibrations δ to the static displacement δ_{st} by a force equal to the amplitude of the harmonic excitation. The greatest amplitude occurs from a disturbance at the blade frequency of 450 Hz $\delta=8\cdot10^{-4}$ m, according to the results of SSS static movement $\delta_{st}=9.29\cdot10^{-5}$ m, thus, the coefficient of dynamic gain at resonance is equal to $\eta\approx8.9$. At a frequency of 400 Hz $\eta\approx1$For pumps, the dynamic coefficient according to [26] can be in the range of 20...25. According to [27] for rotary units, the coefficient n must not exceed 50.

The analysis of the influence of the number of blades on the rotor vibrational activity showed the advantage of the

design of a wheel with eight blades, since the amplitude peak reaches the lowest value for all the investigated frequency cases.

10. Conclusions

1. The computational mechanical scheme for the static calculation of the sixth wheel of a seven-stage centrifugal pump was compiled using the NASTRAN program, the boundary conditions were determined as the pressure values P_5 at the inlet and P_6 at the output of the centrifugal wheel. The computational mechanical scheme for the dynamic calculation of the rotor shaft was compiled using the NASTRAN program, the boundary conditions were determined as values of the hydrodynamic force F_r and the blade frequencies equal to 400 Hz and 450 Hz.

2. The strength calculations for the centrifugal wheel with eight and nine blades have been carried out. The analysis of the results showed the maximum stress in a centrifugal wheel with nine blades equal to σ_{max}=199 MPa, and the stress rate in the wheel with eight blades reached σ_{max}=319 MPa, and both types of the wheel have a sufficient strength coefficient. The amplitude-frequency characteristics of the rotor shaft were determined as follows: at a frequency of 400 Hz the amplitude of deviation from the equilibrium state equals to $\delta=1\cdot10^{-4}$ m and at a frequency of 450 Hz equals to $\delta=8\cdot10^{-4}$ m. The coefficient of dynamic strength coefficient at resonance is equal to $\eta\approx8.9$ at a frequency of 450 Hz and $\eta\approx1$at a frequency of 400 Hz.

3. After comparing the parameters of the static calculation of the centrifugal wheel, it was found that the strength of both wheels with 8 and 9 blades has acceptable values of safety margin. Comparison of the amplitude-frequency response of the rotor shaft, from the influence of the radial force pulsation in the centrifugal wheel indicates an increase in dynamic gain when resonating in a variant with a wheel with 9 blades. That is, the design of the wheel with 9 blades will lead to greater vibration activity of the shaft, which means a decrease in the overall efficiency of the pump. Based on this, when designing the centrifugal wheel, the choice of a design with 8 blades was made.

4. An analysis on the quality of the surface of printed parts has been carried out with 3D technologies so that the preference was given to SLA technology and the surface roughness of the prototype was identified as equal to 3 μm. For further hydrodynamic tests, a prototype of a centrifugal wheel with eight blades has been printed.

References

1. Stel, H., Sirino, T., Ponce, F. J., Chiva, S., Morales, R. E. M. (2015). Numerical investigation of the flow in a multistage electric submersible pump. Journal of Petroleum Science and Engineering, 136, 41–54. doi: https://doi.org/10.1016/j.petrol.2015.10.038
2. Korkmaz, E., Gölcü, M., Kurbanoğlu, C. (2017). Effects of Blade Discharge Angle, Blade Number and Splitter Blade Length on Deep Well Pump Performance. Journal of Applied Fluid Mechanics, 10 (2), 529–540. doi: https://doi.org/10.18869/acadpub.jafm.73.239.26056
3. Liu, H. (2010). Effects of Blade Number on Characteristics of Centrifugal Pumps. Chinese Journal of Mechanical Engineering, 23 (06), 742. doi: https://doi.org/10.3901/cjme.2010.06.742
4. Bai, Y., Kong, F., Xia, B., Liu, Y. (2017). Effect of blade number matching of impeller and diffuser in high-speed rescue pump. Advances in Mechanical Engineering, 9 (5), 168781401770359. doi: https://doi.org/10.1177/1687814017703595
5. Farah, E., Selamat, F., Iskandar, W., Izhan, W. (2018). Design and Analysis of Centrifugal Pump Impeller for Performance Enhancement. Journal of Mechanical Engineering, SI5 (2), 36–53. Available at: https://www.researchgate.net/publication/324690069
6. Tamin, M. N., Hamzah, M. A. (2017). Fatigue Failure Analysis of a Centrifugal Pump Shaft. Failure Analysis and Prevention. doi: https://doi.org/10.5772/intechopen.70672
7. Onari, M. M., Arzani, V. G. (2014). Repetitive Shaft Crack Failure Analysis on a Multistage Centrifugal Pump In Reactor Charge Service In A Nuclear Power Plant - Based On ODS And FEA. Turbomachinery Laboratories. doi: https://doi.org/10.21423/R1D34J
8. Pukhliy, V. A. (2015). To calculation of disks of centrifugal pumps of hydraulic engineering constructions and the atomic power station. Teoriya mehanizmov i mashin, 13, 41–50. Available at: http://tmm.spbstu.ru/25/Pukhliy_25.pdf
9. Zakirnichnaya, M. M., Devyatov, A. R. (2010). Otsenka ekspluatatsionnoy dolgovechnosti rabochih koles tsentrobezhnyh nasosnyh agregatov. Neftegazovoe delo, 2. Available at: http://ogbus.ru/files/ogbus/authors/Zakirnichnaja/Zakirnichnaja_2.pdf
10. Isametova, M., Absadykov, B., Batyrgaliyev, M., Borovik, I. (2018). Centrifugal pump rotor dynamics study. NEWS of National Academy of Sciences of the Republic of Kazakhstan, 5 (431), 226–233. doi: https://doi.org/10.32014/2018.2518-170x.29
11. Zhou, L., Shi, W., Wu, S. (2013). Performance Optimization in a Centrifugal Pump Impeller by Orthogonal Experiment and Numerical Simulation. Advances in Mechanical Engineering, 5, 385809. doi: https://doi.org/10.1155/2013/385809
12. Anofriev, V. Yu., Getsov, L. B., Nozhnitskiy, Yu. A. (2005). Obespechenie prochnostnoy nadezhnosti koles tsentrobezhnyh kompressorov iz vysokoprochnyh staley (Chast' 1). Aviatsionno-kosmicheskaya tehnika i tehnologiya, 6 (22), 16–23. Available at: http://nbuv.gov.ua/UJRN/aktit_2005_6_5
13. Kuzmenko, M. L., Chigrin, V. S., Belova, S. E. (2005). Staticheskaya prochnost' rabochih lopatok i diskov kompressorov i turbin GTD. Rybinsk: RGATA, 74. Available at: http://window.edu.ru/resource/949/76949/files/statika.pdf
14. Sedunin, V. A., Nuss, A. S., Serkov, S. A. (2016). Studying the Strength Characteristics of Axial Compressor Blades. Herald of the Bauman Moscow State Technical University. Series Mechanical Engineering, 3 (108), 90–99. doi: https://doi.org/10.18698/0236-3941-2016-3-90-99
15. Marius, S. (2018). On the durability of progressive cavities pumps. Fiabilitate si Durabilitate – Fiability & Durability, 1, 187–192. Available at: https://www.researchgate.net/publication/325595039

16. Kostyuk, A. G. (2007). Dinamika i prochnost' turbomashin. Moscow: Izdatel'skiy dom MEI, 476. Available at: http://en.bookfi.net/book/651014
17. La Roche-Carrier, N., Dituba Ngoma, G., Ghie, W. (2013). Numerical Investigation of a First Stage of a Multistage Centrifugal Pump: Impeller, Diffuser with Return Vanes, and Casing. ISRN Mechanical Engineering, 2013, 1–15. doi: https://doi.org/10.1155/2013/578072
18. Huang, S., Islam, M. F., Liu, P. (2006). Numerical simulation of 3D turbulent flow through an entire stage in a multistage centrifugal pump. International Journal of Computational Fluid Dynamics, 20 (5), 309–314. doi: https://doi.org/10.1080/10618560600916981
19. Lokalov, G. A., Markovskiy, V. M. (2016). Osevye i tsentrobezhnye nasosy teplovyh elektricheskih stantsiy. Ekaterinburg: Izdatel'stvo Ural'skogo universiteta, 140. Available at: http://hdl.handle.net/10995/40672
20. Zhilkin, V. A. (2013). Azbuka inzhenernyh raschetov v MSC Patran-Nastran-Marc. Sankt-Peterburg: Prospekt Nauki, 574. Available at: http://biblioclub.ru/index.php?page=book&id=565820
21. Zhang, Z. C., Wang, F. J., Yao, Z. F., Leng, H. F., Zhou, P. J. (2013). Investigation on impeller radial force for double-suction centrifugal pump with staggered blade arrangement. IOP Conference Series: Materials Science and Engineering, 52 (3), 032009. doi: https://doi.org/10.1088/1757-899x/52/3/032009
22. Ginesin, L. Yu. (2000). Primenenie MSC.NASTRAN dlya analiza dinamiki rotorov. Moscow: MSCSoftware, 28.
23. Ualiev, G. U., Bisembaev, K., Omirzhanov, Zh. M. (2009). Terbelister teriyasy. Almaty: KazPU im Abaya.
24. Zhang, Y., Hu, S., Zhang, Y., Chen, L. (2014). Optimization and Analysis of Centrifugal Pump considering Fluid-Structure Interaction. The Scientific World Journal, 2014, 1–9. doi: https://doi.org/10.1155/2014/131802
25. Zhao, W. Y., Ge, J. G., Ma, D., Li, C. M., Bao, S. B. (2013). Vibration analysis of large centrifugal pump rotors. IOP Conference Series: Materials Science and Engineering, 52 (2), 022033. doi: https://doi.org/10.1088/1757-899x/52/2/022033
26. Sokolov, E. V. (2008). Modelirovanie i issledovanie dinamicheskih i gidrodinamicheskih protsessov v tsentrobezhnyh nasosah massopodvodyashchih sistem bumagodelatel'nyh mashin. Sankt-Peterburg, 188.
27. Sokolov, E. B., Ankudinov, D. T., Feofanov, A. V. (2006). Dinamicheskie protsessy nagruzheniya detaley tsentrobezhnyh himicheskih nasosov. Nasosy i oborudovanie, 2, 22–24.
28. Zlenko, M. A., Nagaytsev, M. V., Dovbysh, V. M. (2015). Additivnye tehnologii v mashinostroenii. Moscow: GNTS RF FGUP «NAMI», 220.
29. Yan, Y., Li, S., Zhang, R., Lin, F., Wu, R., Lu, Q. et. al. (2009). Rapid prototyping and manufacturing technology: Principle, representative technics, applications, and development trends. Tsinghua Science and Technology, 14 (S1), 1–12. doi: https://doi.org/10.1016/s1007-0214(09)70059-8